Journal of Statistical Mechanics: Theory and Experiment
An IOP and SISSA journal

# Predicting extinction rates in stochastic epidemic models

**Ira B Schwartz**[1], **Lora Billings**[2], **Mark Dykman**[3] and **Alexandra Landsman**[4]

[1] US Naval Research Laboratory, Code 6792, Nonlinear Systems Dynamics Section, Plasma Physics Division, Washington, DC 20375, USA
[2] Department of Mathematical Sciences, Montclair State University, Montclair, NJ 07043, USA
[3] Department of Physics and Astronomy, Michigan State University, East Lansing, MI 48824, USA
[4] Department of Physics and Astronomy, James Madison University, Harrisonburg, VA 22807, USA
E-mail: ira.schwartz@nrl.navy.mil, billingsl@mail.montclair.edu, dykman@pa.msu.edu and landsmax@jmu.edu

Received 27 June 2008
Accepted 17 September 2008
Published 5 January 2009

Online at stacks.iop.org/JSTAT/2009/P01005
doi:10.1088/1742-5468/2009/01/P01005

**Abstract.** We investigate the stochastic extinction processes in a class of epidemic models. Motivated by the process of natural disease extinction in epidemics, we examine the rate of extinction as a function of disease spread. We show that the effective entropic barrier for extinction in a susceptible–infected–susceptible epidemic model displays scaling with the distance to the bifurcation point, with an unusual critical exponent. We make a direct comparison between predictions and numerical simulations. We also consider the effect of non-Gaussian vaccine schedules, and show numerically how the extinction process may be enhanced when the vaccine schedules are Poisson distributed.

**Keywords:** fluctuations (theory), stochastic processes (theory), population dynamics (theory)



1742-5468/09/P01005+12$30.00

## Contents



## 1. Introduction

One of the major goals of the studies of stochastic population dynamics, especially in modeling epidemic spread in a population, is that of predicting finite extinction times when one or more components of the population goes to zero. Practically all diseases of interest exhibit randomness resulting in observed fluctuations. Childhood diseases [1]–[3], meningitis [4], dengue fever and malaria [5] are but a few examples where incidence rates fluctuate with significant amplitude. These fluctuations arise from random contacts within a population, uncertainty in epidemic parameters, and stochastic flux changes from external coupled populations [6, 7]. As diseases evolve in large populations, there is the possibility of finite time extinction and reintroduction of the disease [8, 9]. Extinction occurs where the number of infectives becomes so small that there is insufficient transmission to keep the disease in its endemic state [10]–[12]. Therefore, in the absence of disease reintroduction, the epidemic dies out.

A common mathematical approach to modeling the dynamics of disease spread is to compartmentalize the population into susceptibles ($S$), infectives ($I$), and possibly recovered ($R$). Often it is assumed that there is strong mixing in the system, that is, all species interact with all species, and therefore the species densities do not depend on spatial coordinates. In these models, called SIS or SIR models [13], the disease spread can be characterized by the reproductive rate of infection, $R_0$. In its deterministic form, $R_0$ can be defined so that, for an endemic state to exist along with the disease-free equilibrium (DFE), $R_0 > 1$. When $R_0 < 1$, the DFE is globally stable and the disease becomes extinct. For appropriate parameters where the two states coexist, the DFE is unstable and the endemic state is attracting. In the models we consider here, it is assumed that the endemic state is globally attracting when $R_0 > 1$.

In the presence of random fluctuations, the situation becomes more complicated. Fluctuations cause the disease-free state to be reached, albeit for a limited time, as



J. Stat. Mech. (2009) P01005

indicated by both numerical [14]–[17] and analytic [18, 19, 13, 20, 21] results for various models. Such an extinction process occurs even when $R_0$ is greater than unity.

A major characteristic of fluctuation-induced extinction in the SIS stochastic model for large populations is the extinction rate, or the reciprocal mean first time the number of infectives approaches zero. It has been studied by approximating the full two-dimensional stochastic system (or, more precisely, the system with two dynamical variables) as a continuous one, with fluctuations induced by noise in the Langevin approach. Recently, Doering *et al* [21] investigated a discrete birth–death SIS model and compared it to a continuous model. The analysis referred to a one-variable model, which allows one to obtain an explicit solution in various regimes of $R_0$. However, this model does not reveal some generic features of the full discrete SIS system related to the lack of detailed balance.

It is the purpose of this paper to analyze the general SIS discrete model, and obtain explicit scaling behavior of the extinction rate in the neighborhood of disease onset; i.e., when the reproductive rate is greater than but close to unity. To make clear the assumptions we use for the description of the extinction process, we will include the theory presented in [27]. Using the scaling results, we will compare theory and numerical computations for the extinction rate exponents. Since disease extinction is a goal of vaccine control, and vaccine scheduling is inherently random despite the best policy controls, we numerically examine the case where the vaccine schedule is a Poisson process. A direct comparison between the non-vaccine and vaccine cases will be made numerically.

## 2. The discrete model

We consider a model where susceptibles ($S$) are born at rate $\mu$, both susceptibles and infectives ($I$) die at the same rate $\mu$, and infectives recover at rate $\kappa$ and immediately become susceptible. If susceptibles contact infectives, they may become infected at rate $\beta$. We follow and reproduce the model and notation given in [27].

Since the numbers of susceptibles $S$ and infectives $I$ are integers whereas the events of birth, death, and contact happen at random, we describe the process by the master equation. We introduce vector $\mathbf{X} = (X_1, X_2)$ with components $X_1 = S, X_2 = I$ and vector $\mathbf{r} = (r_1, r_2)$ with integer components $r_1$ and $r_2$, which give, respectively, the increments in $S$ and $I$ in a single transition. The quantity of interest is the probability $\rho(\mathbf{X}, t)$ to have given $S$ and $I$ at time $t$. If transitions are short and uncorrelated, $\mathbf{X}(t)$ is a Markov process, and the evolution of $\rho(\mathbf{X}, t)$ is described by the equation

$$\dot{\rho}(\mathbf{X}, \mathbf{t}) = \sum_r \left[ W(\mathbf{X} - \mathbf{r}; \mathbf{r}) \rho(\mathbf{X} - \mathbf{r}, t) - W(\mathbf{X}; \mathbf{r}) \rho(\mathbf{X}, \mathbf{t}) \right]. \tag{1}$$

In the absence of vaccination the transition rates $W(\mathbf{X}, \mathbf{r})$ are

$$\begin{aligned} &W(\mathbf{X}; (1, 0)) = N\mu, \qquad W(\mathbf{X}; (-1, 0)) = \mu X_1, \\ &W(\mathbf{X}; (0, -1)) = \mu X_2, \qquad W(\mathbf{X}; (1, -1)) = \kappa X_2, \\ &W(\mathbf{X}; (-1, 1)) = \beta X_1 X_2 / N, \end{aligned} \tag{2}$$

where $N$ is the scaling factor which we set equal to the average population, $N \gg 1$.

For sufficiently large $S, I \propto N$, fluctuations of $S, I$ are small on average. If these fluctuations are disregarded, one arrives at the deterministic (mean-field) equations for

the mean values of $S, I$:

$$\begin{aligned}\dot{X}_1 &= N\mu - \mu X_1 + \kappa X_2 - \beta X_1 X_2/N,\\ \dot{X}_2 &= -(\mu+\kappa)X_2 + \beta X_1 X_2/N.\end{aligned} \tag{3}$$

These are standard equations of the SIS model [1]. For $R_0 = \beta/(\mu+\kappa) > 1$ they have a stable solution $\mathbf{X}_\mathrm{A} = N\mathbf{x}_\mathrm{A}$ with $x_{1\mathrm{A}} = R_0^{-1}, x_{2\mathrm{A}} = 1 - R_0^{-1}$. It describes the endemic disease. In addition, (3) have an unstable stationary state (saddle point) $\mathbf{X}_\mathrm{S} = N\mathbf{x}_\mathrm{S}$ with $x_{1\mathrm{S}} = 1, x_{2\mathrm{S}} = 0$. This state corresponds to extinction of infectives.

For $N \gg 1$, the steady state distribution $\rho(\mathbf{X})$ has a peak at the stable state $\mathbf{X}_\mathrm{A}$ with width $\propto N^{1/2}$. This peak is formed over a typical relaxation time $t_\mathrm{r} = \max[\mu^{-1}, (\beta-\mu-\kappa)^{-1}]$, which is much smaller than the extinction time. We are interested in the probability of having a small number infected, $X_2 \ll X_{2\mathrm{A}}$. It is determined by the tail of the distribution. The tail can be approximated by seeking the solution of (1) in the eikonal form,

$$\begin{aligned}&\rho(\mathbf{X}) = \exp[-Ns(\mathbf{x})], \qquad \mathbf{x} = \mathbf{X}/N,\\ &\rho(\mathbf{X}+\mathbf{r}) \approx \rho(\mathbf{X})\exp(-\mathbf{pr}), \qquad \mathbf{p} = \partial_\mathbf{x} s.\end{aligned} \tag{4}$$

For time independent parameters $W$ this formulation was used in a number of papers [20]–[27]. The function $s(x)$ gives the logarithm of the stationary distribution scaled by the average population, and is given by $\dot{s} = -H(\mathbf{x}, \partial_\mathbf{x} s; t)$. The function $s(x)$ is the effective action, and $H$ the auxiliary Hamiltonian.

Following the standard approach of classical mechanics, we can find the action $s(\mathbf{x})$ from classical trajectories of the auxiliary system,

$$\begin{aligned}H(\mathbf{x},\mathbf{p};t) = {}& \mu(e^{p_1}-1) + \mu x_1(e^{-p_1}-1) + \mu x_2(e^{-p_2}-1)\\ &+ \kappa x_2(e^{p_1-p_2}-1) + \beta x_1 x_2(e^{p_2-p_1}-1)\end{aligned} \tag{5}$$

that satisfy equations

$$\dot{\mathbf{x}} = \partial_\mathbf{p} H(\mathbf{x},\mathbf{p};t), \qquad \dot{\mathbf{p}} = -\partial_\mathbf{x} H(\mathbf{x},\mathbf{p};t). \tag{6}$$

## 3. Disease extinction

In this section we analyze the stationary distribution using the eikonal approximation developed in the previous section for the case where fluctuations are from random contacts. We begin by noting that $H = 0$, which in turn is a consequence of the condition $\partial_t s = 0$. The function $s(\mathbf{x})$ has the form [25, 27],

$$s(\mathbf{x}_f) = \int_{-\infty}^{t_f} \mathbf{p}\,\dot{\mathbf{x}}\,\mathrm{d}t, \qquad H(\mathbf{x},\mathbf{p}) = 0. \tag{7}$$

Here, the integral is calculated for a Hamiltonian trajectory $(\mathbf{x}(t), \mathbf{p}(t))$ that starts at $t \to -\infty$ at $\mathbf{x} \to \mathbf{x}_\mathrm{A}, \mathbf{p} \to \mathbf{0}$ and arrives at time $t_f$ at a state $\mathbf{x}_f$. The corresponding trajectory describes the most probable sequence of elementary events $\mathbf{X} \to \mathbf{X}+\mathbf{r}$ bringing the system to $N\mathbf{x}_f$. It provides the absolute minimum to $s(\mathbf{x}_f)$, and $s(\mathbf{x}_f)$ is independent of $t_f$. The quantity $Ns(\mathbf{x})$ gives the exponent in the expression for the mean first-passage time for reaching $N\mathbf{x}$ from the vicinity of the attractor $\mathbf{X}_\mathrm{A}$ [28].



J. Stat. Mech. (2009) P01005

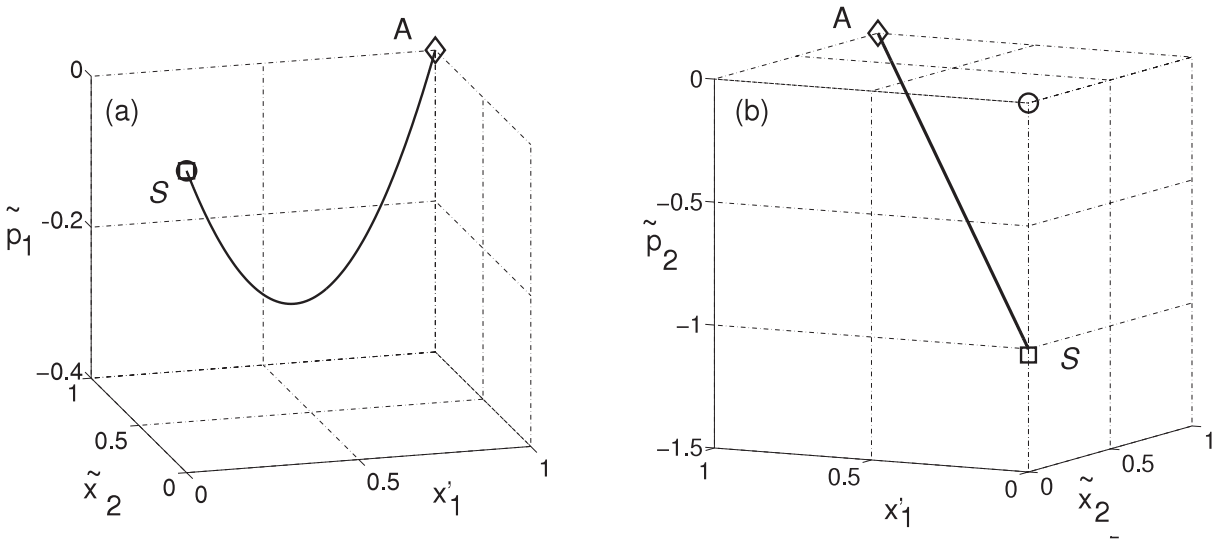


**Figure 1.** 3D projections of the optimal extinction trajectory in (6) and (B.2) in scaled coordinates $\tilde{x}_2 = x_2/(R_0-1), \tilde{p}_2 = p_2/(R_0-1), x'_1 = (1-x_1)/(R_0-1), \tilde{p}_1 = (\mu/\beta)(R_0-1)^2 p_1$. Panels (a) and (b) show $x_1, x_2, p_1$ and $x_1, x_2, p_2$ projections. The trajectory goes from point A that corresponds to the stable state of the system with coordinates $\mathbf{x}_\mathrm{A}$ and zero momentum to point S that corresponds to extinction of the disease, with coordinate $\mathbf{x}_\mathrm{S}$ and with non-zero momentum $\mathbf{p}$.

From equation (4), the extinction rate is determined by $s$ calculated for $x_2 \to 0$, i.e., by the probability density for reaching the disease-free state. It is easy to see that the minimum of $s(\mathbf{x})$ over $x_1$ for $x_2 \to 0$ is reached at the saddle point $\mathbf{x}_\mathrm{S}$ of the fluctuation-free motion. Thus the entropic barrier for extinction is $Ns_\mathrm{ext} = Ns(\mathbf{x}_\mathrm{S})$, and the typical extinction time is $\tau \propto \exp(Ns_\mathrm{ext})$.

The Hamiltonian trajectory $\mathbf{x}_\mathrm{ext}(t), \mathbf{p}_\mathrm{ext}(t)$ that gives $s(\mathbf{x}_\mathrm{A})$ is the optimal extinction trajectory. One can show that it approaches $\mathbf{x}_\mathrm{A}$ as $t \to \infty$. This is similar to other problems of an optimal trajectory leading from a deterministic stable state to a saddle point [25, 29]. However, in contrast to the more common situation, for $t \to \infty$ the momentum $\mathbf{p}_\mathrm{ext}$ does not go to zero. Instead $\mathbf{p}_\mathrm{ext}(t) \to \mathbf{p}_\mathrm{S}$, with $\mathbf{p}_\mathrm{S} = (0, -\ln R_0)$. This is in spite of the fact that, along with $(\mathbf{x}_\mathrm{S}, \mathbf{p}_\mathrm{S})$, the Hamiltonian $H$ has a 'standard' fixed point $(\mathbf{x}_\mathrm{S}, \mathbf{p} = \mathbf{0})$. A proof is given in appendix A.

An explicit analytical solution for the Hamiltonian trajectories can be obtained close to a bifurcation point where the number of the stationary solutions of the deterministic equations changes [25, 27]. In the present case it corresponds to $0 < \eta \ll 1, \eta = \beta - \mu - \kappa \equiv \beta(R_0-1)/R_0$. For $\eta \ll 1$ the mean-field value of $x_2$ in the stable state $x_{2\mathrm{A}} = \eta/\beta \ll 1$ is close to $x_{2S}$. The relaxation time of $x_2$ near the stable state is $\eta^{-1}$. It is much longer than the relaxation time of $x_1$, which is $\mu^{-1}$, i.e., $x_2$ is a soft mode. Coordinate $x_1$ follows $x_2$ adiabatically on the timescale that largely exceeds $\mu^{-1}$. See appendix B for details.

The solution (B.2) in appendix B describes in particular the optimal extinction trajectory as depicted in figure 1. The full Hamiltonian equations (5) and (6) were also solved numerically to get the optimal path from the attractor to the extinct state. The solution is compared with the adiabatic solution in figure 2, where the control parameter, $\eta$, is small.



J. Stat. Mech. (2009) P01005

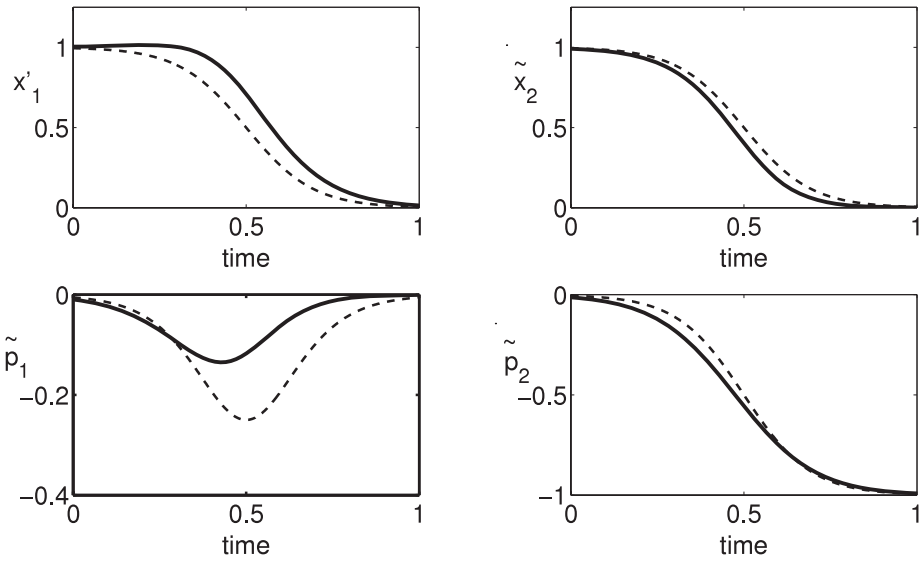


**Figure 2.** Time series of the heteroclinic orbits. The time series in bold represents those of the adiabatic equations in (B.2). The dashed lines were computed using the full Hamiltonian system (6), where time was scaled to the period of a long period approximating orbit to the heteroclinic orbit. The parameter values in the numerical computations were $\mu = 0.02$, $\kappa = 100.0$, $\beta = 100.05$, $\eta = 0.0308$.

From (7) and (B.2), we derive one of our main results,

$$s_{\text{ext}} = s(\mathbf{x}_{\text{S}}) = \eta^2/2\beta^2 = (R_0 - 1)^2/2R_0^2. \tag{8}$$

The entropic barrier for extinction $Ns_{\text{ext}}$ scales with the distance to the bifurcation point $\eta \propto R_0 - 1$ as $\eta^2$. This is in contrast to the case for standard scaling of the activation energy of escape near a saddle–node bifurcation point, where the critical exponent is 3/2 [25]. Such unusual scaling is related to $\mathbf{p}_{\text{S}}$ being non-zero. It emerges also in the SIR model [30].

## 4. Numerical simulations

In this section, we wish to compute the effective exponents which yield the scaling dependence on $R_0$ given in (8). Following the Monte Carlo algorithm in [31], we simulate the system described by the master equations (1) and (2) for a population of size $N$. In figure 3, the data represents the average time to extinction, $\tau$, over 1000 realizations. Black dots denote the mean for a given $R_0$ over the range of population sizes listed in the caption, and the error bars measure deviation from the mean in the data. To compare and contrast the change in the extinction time over the range of $R_0$, we have shifted the data vertically by 0.0675 to overlay the results from (8) where $R_0 - 1$ is small. For small $R_0 - 1$, the asymptotic scaling theory and numerical results for the exponent of the extinction rates agree. The actual range of agreement occurs up to $R_0 \approx 2$, after which the results begin to deviate from the asymptotic theory.

Numerically, the simulations may be used to explore the geometry of the path to extinction in the two-dimensional SIS model. For each run, we examine trajectories



J. Stat. Mech. (2009) P01005

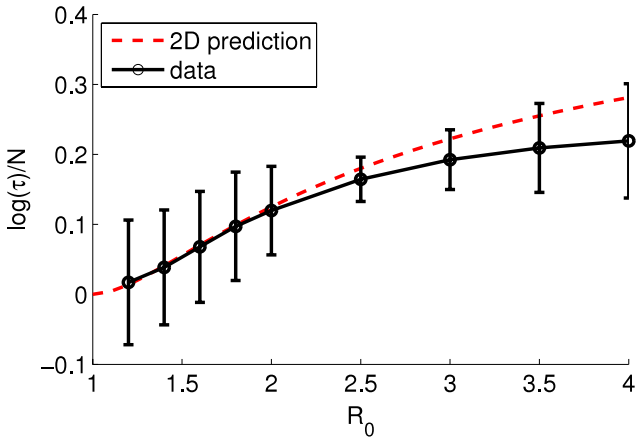


**Figure 3.** The logarithm of the extinction time $\tau$ scaled by the population size, $N$. Black dots are the average over $N$ of $\log(\tau)$. The dashed line is the extrapolation of equation (8). The fixed parameters are: $\mu = 0.02$ (1/year), $\kappa = 100$ (1/year), and $N = 20, 30, 40, 50, 60, 70, 80$ (people). We vary $\beta$ to adjust $R_0$.

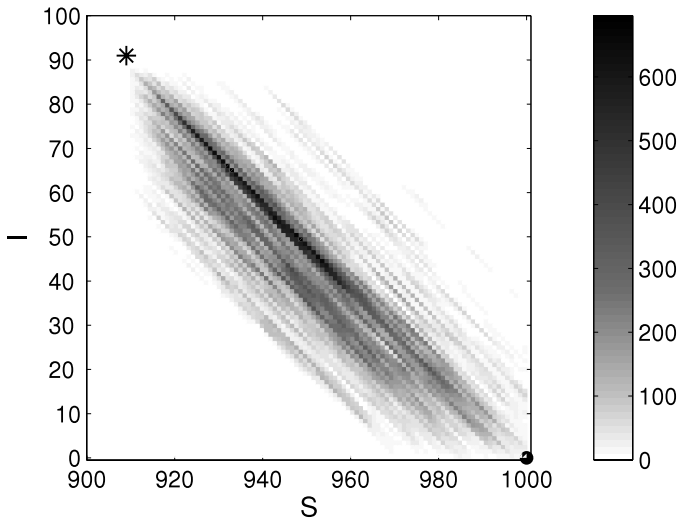


**Figure 4.** A pre-history histogram plot in the state space of $(S, I)$. The endemic state is represented by the star, while the filled circle locates the DFE. The grayscale denotes the number of points that occur at a given discrete value of $(S, I)$ over 5000 realizations. The segment of the optimal path to extinction can be seen along the peak of the distribution. Parameters: $\mu = 0.02$ (1/year), $\beta = 110$ (1/year), $\kappa = 100$ (1/year), and $N = 1000$ (people).

leading to extinction at the DFE. We then reverse time along the orbit until we reach a neighborhood of the endemic state. In figure 4, a plot is shown of the averaged pre-history realizations projected onto $(S, I)$ state space. Notice in the figure that the peak of the distribution lies along a curve approximating the optimal path segment from the endemic state to the DFE, given by the adiabatic approximation in normalized coordinates as $x_2 = 1 - x_1$.

J. Stat. Mech. (2009) P01005

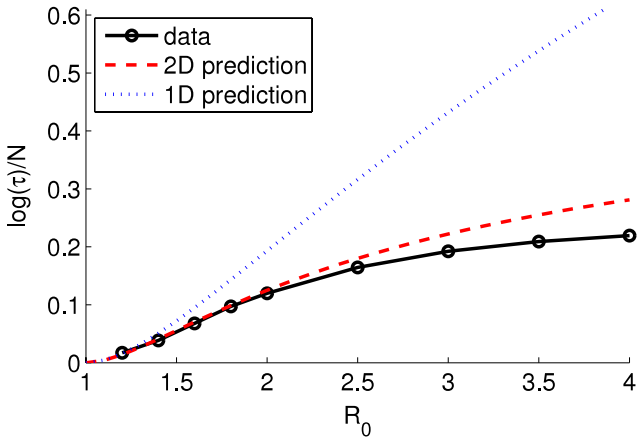


**Figure 5.** A comparison of theoretical extinction time predictions between one- and two-dimensional SIS models. The black dots are numerically simulated as in figure 3. The dashed (red) line is given by equation (8) for the two-dimensional SIS model extrapolated to the range of non-small $R_0 - 1$. The dotted (blue) line is the prediction of [21].

## 5. Conclusions and discussion

To summarize, we have considered fluctuations in the full two-variable SIS model and found the rate of extinction. The problem has been reduced to the analysis of dynamics of an auxiliary Hamiltonian system, with non-trivial boundary conditions. Where the reproductive rate of infection $R_0$ is close to 1, the extinction rate displays scaling with $R_0$ with the logarithm of the rate being $\propto (R_0 - 1)^2$.

An interesting feature that we have found is that, as $R_0$ increases, the normalized extinction barrier $s_{\rm ext}$ grows much more slowly than in the one-dimensional SIS, where $s_{\rm ext}$ scales as $\log R_0$ [21]. In figure 5 we compare the one-and two-dimensional theoretical extinction results with the mean of the data presented in figure 3. Clearly, the difference between one- and two-dimensional systems becomes significant already for $R_0 > 2$.

One of the important results that our research provides is the general theoretical framework that can be used to measure how vaccines may enhance extinction rates. In particular, the scaling laws can be used specifically to compare extinction rates in the presence of fine resources. For example, it may be possible to vaccinate a limited fraction of new susceptibles every year, but maybe apply it more frequently. Conversely, it may be possible to implement one mass vaccination per year (a current approach for most childhood diseases). Other approaches for 'slow' diseases may require vaccination that is intermittent.

Vaccination is intrinsically random. We model it by a Poisson process. The vaccine modifies the transition rate of susceptibles, now given by $W(\mathbf{X}; (1, 0)) = N[\mu - \xi(t)]$. The time dependent vaccination of incoming susceptibles reduces their probability to become infected at rate $\xi(t)$.

In simulating a vaccination event in a finite population, we use a Poisson distribution of short rectangular pulses with intensity (area under the pulse) $g$ and frequency $\nu$.

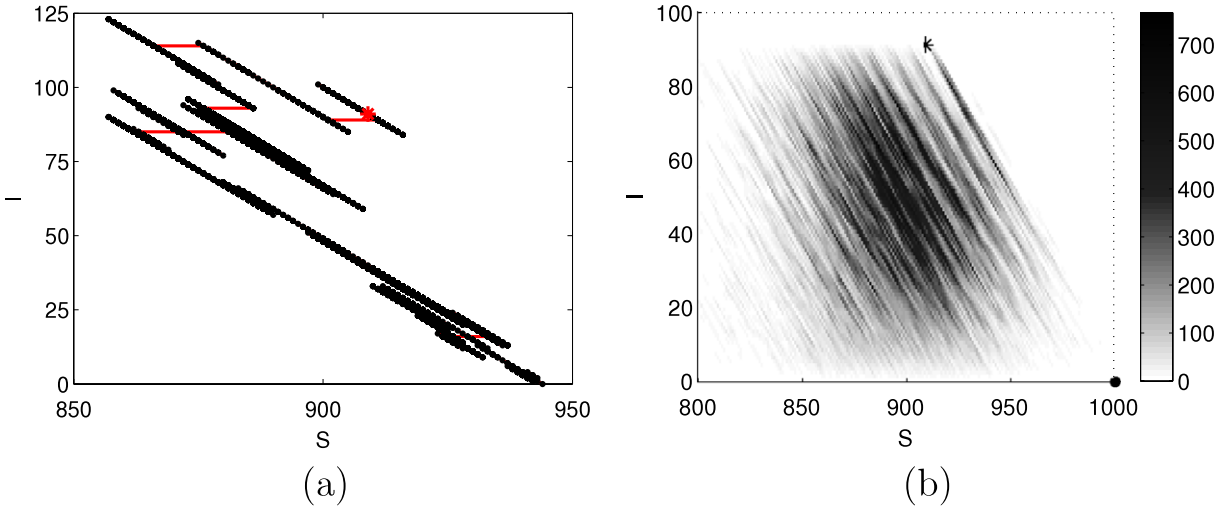


**Figure 6.** (a) A simulation (black dots) of an extinction event in the presence of vaccination. The epidemic parameters are the same as in figure 4 and the vaccine parameters are $gN = 10$ and $\nu = 12$. The vaccination pulses shift the times series left, as shown by the horizontal lines. The (red) star shows the location endemic state. (b) The corresponding histogram plot of response to vaccine in state space of $(S, I)$ over 1000 realizations.

That is, the number of people removed from the incoming susceptible population per pulse is $gN$. A sample trajectory is depicted in figure 6. We use the same epidemiological parameters as in figure 4, with vaccine parameters $gN = 10$ and $\nu = 12$ per year. As before, we examined the pre-history of the trajectories leading to extinction averaged over 1000 realizations. We note that, even where we look at a trajectory that leads to extinction and starts near the endemic state, it spends a comparatively long time near the endemic state going back and forth. For convenience, we examine the pre-history up to the last time the infectives reach a threshold that corresponds to the endemic state. The results are depicted in figure 6. Notice that the mean paths to extinction show the effect of reducing the susceptibles discretely. That is, every time the vaccine is pulsed to remove a fraction of the population, the pre-history curves are shifted to the left. The result is a population with fewer susceptibles, and therefore, the mean time to extinction is reduced.

Generalizing over a range of frequency and vaccine amplitude, we can quantify how strongly the vaccine enhances the extinction rate. The ratio of the mean extinction times without and with the vaccine gives the vaccine extinction factor $A_{\text{ext}}$. The results are displayed in figure 7. As expected, more frequent vaccinations at higher removal rates increase the rate of extinction, as illustrated by the increase in extinction factor. For slowly propagating diseases where $R_0 - 1$ is small, an explicit expression for the extinction factor can be obtained [27].

In conclusion, we have shown that the problem of extinction in a finite population SIS model may be analyzed using an optimal path approach. In the absence of vaccination, we have shown analytically that the effective entropic barrier for extinction scales as the square of the distance to the bifurcation point. In the presence of vaccination, we have

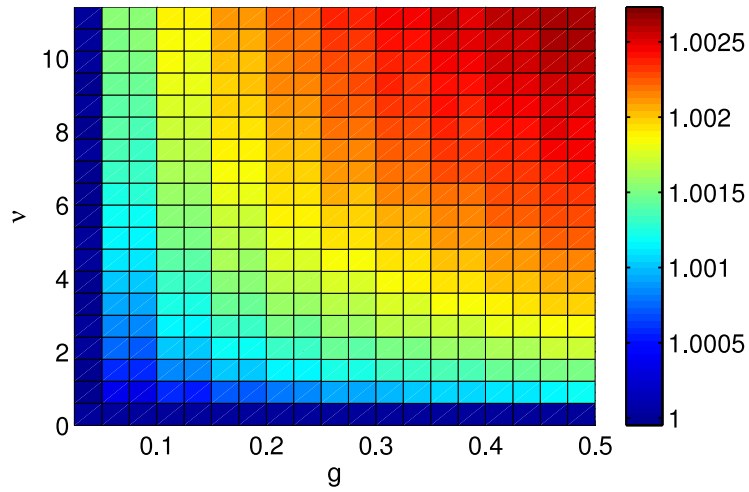


**Figure 7.** Vaccine-induced change of the entropic barrier for extinction $(\log A_{\text{ext}})/N$ computed using the Monte Carlo simulation from. The parameters used are $\mu = 0.02$, $\kappa = 100.0$, $\beta = 110.0$, $N = 1000$.

defined and computed an extinction factor, which measures the increased rate of extinction as a function of the Poisson frequency and amplitude of vaccination.

The current model used for analysis is an overdamped vector field. Future work based on the current analytical and numerical schemes will be extended to more general models such as SIR, SEIR, and MSI models [32], which are typically underdamped. Other aspects critical to understanding the vaccine application are models of epidemic spread in seasonally changing environments, and we will extend our results to those as well. These are challenging problems of noise in the important area of understanding and control of epidemics.

## Acknowledgments

The authors are grateful to A Kamenev and B Meerson for valuable discussions. This work was supported in part by the Army Research Office, Office of Naval Research, and the Armed Forces Medical Center. LB is supported by ARO W911NF-06-1-0320 and NSF DMS-0414087, MD is supported by the ARO through grant No W911NF-06-1-0324.

## Appendix A

In this appendix we show that the occurrence of an optimal extinction path with non-zero momentum at the extinction state is indeed a feature of the system under consideration. We note that the optimal extinction trajectory should lie on the stable manifold of the appropriate fixed point. It is straightforward to show that the stable manifold of the 'wrong' fixed point $(\mathbf{x}_S, \mathbf{p} = \mathbf{0})$ lies in the plane $x_2 = p_1 = 0$. An optimal path does not reach this plane in finite time. From (6), $x_2$ approaches zero exponentially as $t \to \infty$, but for $t \to \infty$ the system as a whole approaches a fixed point. Therefore the optimal extinction trajectory does not lie on the stable manifold of $(\mathbf{x}_S, \mathbf{p} = \mathbf{0})$. It may only lie

on the stable manifold of the fixed point $(\mathbf{x}_S, \mathbf{p}_S)$, which is not confined to a plane in the $(\mathbf{x}, \mathbf{p})$ space. An alternative argument is provided in [27].

The situation where an auxiliary Hamiltonian system has two fixed points with the same $\mathbf{x}_S$ was first noticed for a system described by the Fokker–Planck equation with a singular diffusion matrix at $\mathbf{x}_S$ [18], and the 'right' point was chosen on the basis of numerical simulations. This situation was also found for a system described by a one-variable master equation, where the Hamiltonian dynamics is integrable [20]; it occurs also in a two-variable susceptible–infected–recovered (SIR) model concurrently studied by Kamenev and Meerson [30].

## Appendix B

The solution of Hamiltonian equations (6) in the adiabatic approximation is simplified by the fact that $x_2 \ll 1$ and $|p_2| \ll 1$. To leading order in $\eta$ we have $x_1 = 1 - x_2, p_1 = \beta x_2 p_2/\mu$, while the equations for slow variables $x_2, p_2$ have the Hamiltonian form

$$\dot{x}_2 = \partial H^{\mathrm{ad}}/\partial p_2, \qquad \dot{p}_2 = -\partial H^{\mathrm{ad}}/\partial x_2, \tag{B.1}$$

with Hamiltonian $H^{\mathrm{ad}} = \eta x_2 p_2 - \beta x_2 p_2 (x_2 - p_2)$. The Hamiltonian trajectory is

$$p_2(t) = x_2(t) - \frac{\eta}{\beta}, \qquad x_2(t) = x_{2\mathrm{A}} \left(1 + e^{\eta(t-t_0)}\right)^{-1}. \tag{B.2}$$

## References


[1] Anderson R M and May R M, 1991 *Infectious Diseases of Humans—Dynamics and Control* (Oxford: Oxford Science Publications)

[2] Bolker B M and Grenfell B T, *Chaos and biological complexity in measles dynamics*, 1993 *Proc. R. Soc. Lond.* B **251** 75

[3] Bolker B M, *Chaos and complexity in measles models—a comparative numerical study*, 1993 *IMA J. Math. Appl. Med.* **10** 83

[4] Patz J, *A human disease indicator for the effects recent global climate change*, 2002 *Proc. Nat. Acad. Sci.* **99** 12506

[5] Patz J, Hulme M, Rosenzweig C, Mitchell T, Goldberg R, Githeko A, Lele S, McMichael A and Le Sueur D, *Climate change: regional warming and malaria resurgence*, 2002 *Nature* **420** 627

[6] Rand D A and Wilson H B, *Chaotic stochasticity: a ubiquitous source of unpredictability in epidemics*, 1991 *Proc. R. Soc. Lond.* B **246** 179

[7] Billings L, Bollt E M and Schwartz I B, *Phase-space transport of stochastic chaos in population dynamics of virus spread*, 2002 *Phys. Rev. Lett.* **88** 234101

[8] Andersson H and Britton T, *Stochastic epidemics in dynamic populations: quasi-stationarity and extinction*, 2000 *J. Math. Biol.* **41** 559

[9] Cummings D A T, Irizarry R A, Huang N E, Endy T P, Nisalak A, Ungchusak K and Burke D S, *Travelling waves in the occurrence of dengue haemorrhagic fever in Thailand*, 2004 *Nature* **427** 344

[10] Keeling M J, 2004 *Ecology, Genetics, and Evolution* (New York: Elsevier)

[11] Verdasca J A, da Gama M M T, Nunes A and Bernardino N R, *Recurrent epidemics in small world networks*, 2005 *J. Theor. Biol.* **233** 553

[12] Bartlett M S, *Some evolutionary stochastic processes*, 1949 *J. R. Statist. Soc.* B **11** 211

[13] Jacquez J A and Simon C P, *The stochastic si model with recruitment and deaths. 1. Comparison with the closed sis model*, 1993 *Math. Biosci.* **117** 77

[14] West R W and Thompson J R, *Models for the simple epidemic*, 1997 *Math. Biosci.* **141** 29

[15] Nasell I, *On the quasi-stationary distribution of the stochastic logistic epidemic*, 1999 *Math. Biosci.* **156** 21

[16] Billings L and Schwartz I B, *A unified prediction of computer virus spread in connected networks*, 2002 *Phys. Lett.* A **297** 261




J. Stat. Mech. (2009) P01005

[17] Cummings D A T, Schwartz I B, Billings L, Shaw L B and Burke D S, *Dynamic effects of antibody-dependent enhancement on the fitness of viruses*, 2005 *Proc. Nat. Acad. Sci.* **102** 15259
[18] van Herwaarden O A and Grasman J, *Stochastic epidemics, major outbreaks and the duration of the endemic period*, 1995 *J. Math. Biol.* **33** 581
[19] Allen L J S and Burgin A M, *Comparison of deterministic and stochastic sis and sir models in discrete time*, 2000 *Math. Biosci.* **163** 1
[20] Elgart V and Kamenev A, *Rare event statistics in reaction–diffusion systems*, 2004 *Phys. Rev.* E **70** 041106
[21] Doering C R, Sargsyan K V and Sander L M, *Extinction times for birth–death processes: exact results, continuum asymptotics, and the failure of the Fokker–Planck approximation*, 2005 *Multiscale Modeling Simul.* **3** 283
[22] Kubo R, Matsuo K and Kitahara K, *Fluctuation and relaxation of macrovariables*, 1973 *J. Stat. Phys.* **9** 51
[23] Ventcel' A D, *Rough limit theorems on large deviations for Markov random processes. I*, 1976 *Teor. Verojatn. Primen.* **21** 235
[24] Hu G, *Stationary solution of master-equations in the large-system-size limit*, 1987 *Phys. Rev.* A **36** 5782
[25] Dykman M I, Mori E, Ross J and Hunt P M, *Large fluctuations and optimal paths in chemical-kinetics*, 1994 *J. Chem. Phys.* **100** 5735
[26] Tretiakov O A, Gramespacher T and Matveev K A, *Lifetime of metastable states in resonant tunneling structures*, 2003 *Phys. Rev.* B **67** 073303
[27] Dykman M I, Schwartz I B and Landsman A, *Disease extinction in the presence of non-Gaussian noise*, 2008 *Phys. Rev. Lett.* **101** 078101
[28] Matkowsky B J, Schuss Z, Knessl C, Tier C and Mangel M, *Asymptotic solution of the Kramers–Moyal equation and first-passage times for markov jump processes*, 1984 *Phys. Rev.* A **29** 3359
[29] Maier R S and Stein D L, *Limiting exit location distributions in the stochastic exit problem*, 1997 *SIAM J. Appl. Math.* **57** 752
[30] Kamenev A and Meerson B, *Extinction of the infectious disease: a large fluctuation in a nonequilibrium system*, 2008 *Phys. Rev.* E **77** 061107
[31] Gillespie D T, *Exact stochastic simulation of coupled chemical-reactions*, 1977 *Papers of the American Chemical Society* vol 173 p 128 (Abstract)
[32] Billings L and Schwartz I B, *Exciting chaos with noise: unexpected dynamics in epidemic outbreaks*, 2002 *J. Math. Biol.* **44** 31

J. Stat. Mech. (2009) P01005